

Catalyst Enhancement and Recyclability by Immobilization of Metal Complexes onto Graphene Surface by Noncovalent Interactions

Sara Sabater, Jose A. Mata,* and Eduardo Peris*

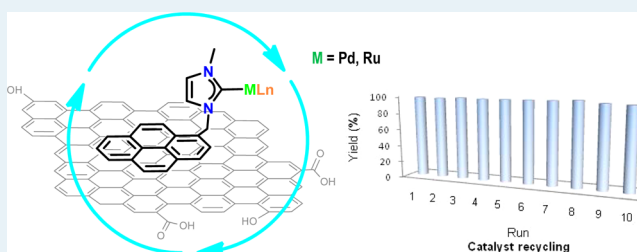
Departamento de Química Inorgánica y Orgánica, Universitat Jaume I, Avda. Sos Baynat s/n, 12071 Castellón de la Plana, Castellón, Spain

Supporting Information

ABSTRACT: The immobilization of a homogeneous catalyst onto a solid surface is one of the major challenges in catalysis, because it may facilitate the separation of the catalyst and the reaction products and may also give rise to the reutilization of the catalyst in multiple subsequent cycles. Noncovalent interactions between the catalyst and the support are arising as interesting alternatives to the more widely used covalent interactions, because they avoid the functionalization of both the catalyst and the surface, which may in turn lead to the modification of the inherent properties of the catalyst.

However, some other problems may arise, such as leaching. In this work, we have obtained two complexes containing an N-heterocyclic carbene ligand with a pyrene tag, which we immobilized onto the surface of reduced graphene oxide (rGO), by π -stacking. The catalytic properties of the parent molecular complexes and hybrid materials have been studied in the palladium-catalyzed hydrogenation of alkenes and the ruthenium-catalyzed alcohol oxidation. The results show that the catalytic properties are improved in the hybrid materials, compared to the catalytic outcomes provided by the homogeneous analogues. Although the palladium-catalyzed reactions may be due to the formation of Pd nanoparticles, the ruthenium-catalyzed ones are facilitated by the supported molecular catalyst. The catalyst stability was analyzed by means of recyclability studies, hot filtration test, and large-scale experiments. Both hybrid materials have been reused up to 10 times without any decrease in activity, affording quantitative yield of products. The hot filtration experiment reveals that the catalysis is heterogeneous in nature without any detectable leaching or boomerang effect. The work constitutes a clear improvement over other known immobilization methodologies and offers a practical methodology which may inspire future developments of efficient heterogenized catalysts.

KEYWORDS: hydrogenation, alcohol oxidation, graphene, ruthenium, palladium, N-heterocyclic carbenes



INTRODUCTION

Despite the attractive properties of many homogeneous catalysts in terms of activity and selectivity, they suffer from difficulties associated with separating the products from the catalyst,¹ an important drawback that causes industries to be relatively reluctant to use them for the large-scale production of materials. Another important drawback for the industrial use of homogeneous catalysts concerns catalyst recycling, for which an enormous effort in the immobilization of known catalysts onto solid supports is currently being carried out.² The main goal in recycling a catalyst refers to achieving consistent high yields in repeated runs that confirm the robustness of the supported catalytic system, a necessary requirement for long-term applications. Undoubtedly, the most widely used method for the immobilization of a homogeneous catalyst is the formation of a covalent bond between the solid support and the ligand. This general method has two important drawbacks: first, arising from the need for an additional functionalization of the catalyst ligand and solid surface (which in turn implies an increase in the catalyst preparation cost) and second, arising from the possible changes in chemical reactivity (and therefore in catalytic activity) derived from the formation of the covalent

bond between the support and the catalyst. As an alternative, noncovalent interactions are emerging as a powerful tool that gives rise to supported catalysts without chemical modification of the homogeneous catalyst, although the stability against leaching may become a problem that needs to be avoided by the careful selection of the reaction conditions, immobilization method, nature of the support, and catalytic complex.^{2d}

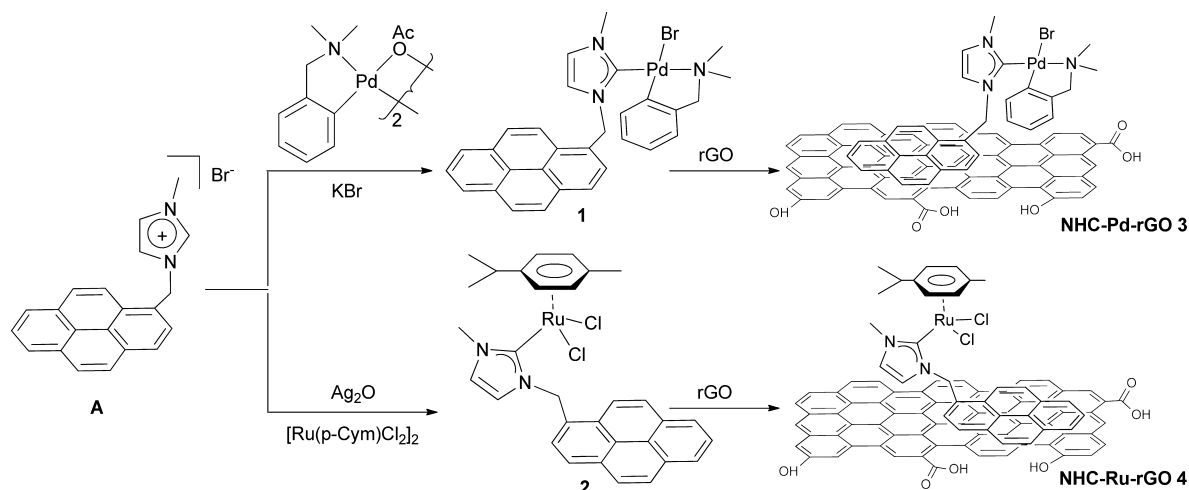
Graphene and derivatives have attracted increasing attention because of their unique physical and chemical properties,³ which make them particularly interesting in the fields of nanochemistry and catalysis.⁴ Chemically derived graphenes (CDGs) such as graphene oxide (GO) and reduced graphene oxide (rGO), are ideal candidates for immobilization due to their inertness, large surface area, stability, and availability. In fact, graphene derivatives have recently been used as supports for the covalent immobilization of homogeneous catalysts.⁵ Together with their inherent properties, graphene and derivatives offer a unique opportunity to noncovalent

Received: March 25, 2014

Revised: May 13, 2014

Published: May 14, 2014

Scheme 1. Synthesis of Hybrid Materials



modifications by π -stacking interactions with molecules containing polycyclic aromatic hydrocarbons,⁶ from which pyrene-functionalized systems constitute promising examples.⁷ Also, and very important is the fact that the immobilization of polyaromatic hydrocarbons onto rGO does not depend on the pH of the solution.^{7a} From these basic ideas, it becomes rather obvious that one potentially effective form for catalyst heterogenization would be the preparation of pyrene-containing catalysts, which could be noncovalently supported onto a graphene surface. Pyrene-containing metal complexes have been already supported onto graphene derivatives, proving to be a versatile way of functionalization of nanostructured graphitic materials,⁸ and they have even been used in catalysis proving interesting recyclability properties.⁹ The noncovalent interaction between the pyrene and rGO is based on van der Waals forces (π -stacking), and it is controlled by thermodynamics.¹⁰ This type of rGO functionalization is particularly attractive, because it offers the possibility of attaching metal complex without affecting the electronic network. For the choice of the suitable catalyst, N-heterocyclic carbene-based complexes seem to be good candidates, due to the σ -donor capacity of NHC ligands and the stability of the metal complexes derived that make them suitable to operate under harsh reaction conditions.¹¹ On the basis of all these arguments, we now describe the synthesis of an imidazolium salt with a pyrene tag that allows the preparation of palladium and ruthenium complexes that have been immobilized onto the rGO surface by π -stacking interactions. We have studied the catalytic properties of these new hybrid materials in the ruthenium-catalyzed oxidation of alcohols and in the palladium-mediated hydrogenation of a wide set of organic molecules. In both reactions, we were glad to observe that the supported catalysts displayed higher activities than the homogeneous related complexes, and the heterogeneized catalysts were recycled 10 times without loss of activity.

RESULTS AND DISCUSSION

The imidazolium salt **A** was obtained by alkylation of methylimidazole using commercially available 1-(bromomethyl)pyrene. The reaction of **A** with the palladacycle dimer $[\text{Pd}(\text{dmba})\text{OAc}]_2$ (dmba = cyclo-orthometalated *N,N*-dimethyl benzylamine) in the presence of KBr affords the corresponding NHC-Pd(II) complex **1** in 60% yield (Scheme 1). The NHC-

Ru(II) complex **2** was obtained starting from the imidazolium salt **A** by transmetallating the NHC from the corresponding Ag-NHC complex, which was generated and used in situ by reaction of the imidazolium salt with Ag_2O . Both the palladium and ruthenium complexes are air-stable in the solid state and in solution. Complexes **1** and **2** were characterized by NMR spectroscopy, mass spectrometry, and elemental analysis. The ^1H NMR spectra of complexes **1** and **2** confirm the disappearance of the acidic signal of the imidazolium salt at 9.21 ppm, suggesting a carbene-type bonding of the imidazolylidene ligand. A more concluding evidence is obtained from the ^{13}C NMR, which shows the characteristic signals of the $\text{M}-\text{C}_{\text{carbene}}$ at 172.9 ppm for **1** and 174.8 ppm for **2**. Positive ion electrospray mass spectra analysis (ESI-MS) for complexes **1** and **2** in MeCN showed an intense peak for $[\text{M} - \text{X}]^+$ at $m/z = 536.3$ and $m/z = 567.2$, respectively, which confirm the proposed molecular composition of the complexes based on the mass/charge relation and the isotopic pattern (see Supporting Information for details).

The molecular structure of compound **1** was confirmed by means of X-ray diffractometry. The structure analysis reveals a palladium center with a bromide, the NHC ligand, and the chelating bound *N,N*-dimethylbenzylamine in a square-planar coordination environment (Figure 1). The C–N orthometalated amine forms a five-membered ring that adopts an envelope conformation. The Pd– $\text{C}_{\text{carbene}}$ distance measures 1.970(8) Å. The packing diagram of complex **1** shows an intermolecular slipped π -stacking between pairs of molecules (interplanar distance 3.6 Å) indicating the tendency of the pyrene moiety to display this type of noncovalent interaction.¹²

Complexes **1** and **2** were supported onto reduced graphene oxide (rGO) by mixing the molecular complexes and the rGO material in dichloromethane in an ultrasound bath for 30 min and stirring for 10 h. The first evidence that molecular complexes **1** and **2** were anchored over the surface of rGO arises from the disappearance of the color of the solution. The yellow solution of complex **1** in dichloromethane disappears as the complex is retained on the rGO. The palladium-containing material, NHC-Pd-rGO (**3**), was filtered and washed with dichloromethane. The ^1H NMR spectrum of the filtrate revealed the absence of any trace of **1** in the solution and therefore provided us with the first evidence of the quantitative deposition of **1** onto rGO. The exact palladium content on **3**

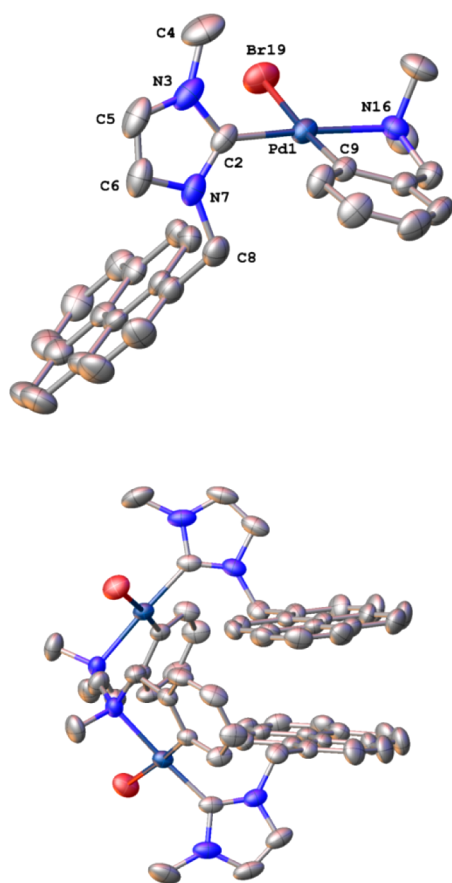


Figure 1. Molecular (top) and packing (down) diagrams showing the π -stacking of complex 1. Ellipsoids at 50% probability level. Hydrogens omitted for clarity. Selected bond lengths (Å) and angles ($^\circ$): Pd(1)–C(2) 1.978(3), Pd(1)–C(9) 2.002(3), Pd(1)–Br(19) 2.5435(7), Pd(1)–N(16) 2.138(3), C(2)–N(7) 1.343(5), N(7)–C(8) 1.471(4), Br(19)–Pd(1)–C(2) 92.99(8), Br(19)–Pd(1)–N(16) 93.25(7), N(16)–Pd(1)–C(9) 83.00(11), C(9)–Pd(1)–C(2) 90.77(12), Br(19)–Pd(1)–C(2)–N(3) 67.5. The π -stacking interplanar distance measures 3.6 Å.

was determined by digestion of the samples in hot HCl/HNO₃ followed by ICP-MS analysis. The results obtained accounted for a 9.3 wt % of 1 in 3. The ruthenium complex 2 was anchored over the rGO using the same procedure, and the ICP-MS analysis accounted for a 9.0 wt % of complex in the hybrid material NHC-Ru-rGO (4). We did not observe desorption of the compounds 1 or 2 from the rGO when changing the solvent polarity or by increasing the temperature in the catalytic experiments carried out (*vide infra*). In order to confirm that the pyrene fragment is responsible for the grafting of the molecular complexes on the graphene surface, we performed a control experiment, in which we applied the same grafting experiment using the pyrene-free complex [RuCl₂(I_nBu)(*p*-cymene)]¹³ (I_nBu = 1,3-di-*n*-butylimidazolyldiene), and we observed that, under exactly the same conditions, the molecular complex quantitatively remained in the solution, thus confirming that the pyrene fragment is responsible for the adsorption of the complex to the surface of the solid.

The characterization of the hybrid materials 3 and 4 was performed using UV–vis, FTIR, Raman, SEM, and HRTEM (see Supporting Information for details). The FTIR spectra of NHC-Pd-rGO (3) and NHC-Ru-rGO (4) displayed hardly evident additional peaks compared to that shown by rGO, due

to the weak signal and overlapping of absorption by other groups present in the support (Figures S3 and S4). On the other hand, UV–vis measurements (Figures S1 and S2) reveal that the spectra of the hybrid materials consist of the overlap of the molecular complexes (1 or 2) with rGO, clearly confirming the presence of the complex on the rGO, as seen by the pyrene UV–vis characteristic signals.^{9b,14} The Raman spectrum of rGO shows the two prominent peaks at 1350 and 1592 cm⁻¹, which are attributed to D and G bands, respectively (Figure S5).¹⁵ The incorporation of the NHC-Pd and NHC-Ru complexes show a slight blue shift of the G band (1594 cm⁻¹, for both 3 and 4), which may be attributed to the π -stacking of the pyrene fragment onto the rGO layer.¹⁶ The analysis of the surface area of both materials was performed by argon sorption analysis at 77 K. The BET area for 3 and 4 was 262 and 238 m² g⁻¹, respectively, significantly lower than that shown by the rGO raw material (456 m² g⁻¹).

The elemental mapping by energy-dispersive X-ray spectroscopic analysis (EDS) performed by means of HRTEM of 3 and 4, confirmed the homogeneous distribution of palladium and ruthenium in the two hybrid materials (Figure 2).

In order to study the catalytic activity of the hybrid materials NHC-Pd-rGO (3) and NHC-Ru-rGO (4), we decided to test the materials in two benchmark reactions typically catalyzed by Pd and Ru. The palladium-containing material, 3, was tested in the hydrogenation of unsaturated organic substrates using molecular hydrogen,¹⁷ whereas the ruthenium-containing material, 4, was tested in the dehydrogenation of alcohols.¹⁸ The palladium-catalyzed reduction of alkenes was performed in toluene in the presence of Cs₂CO₃ at 100 °C using H₂ (1 atm) with a catalyst loading of 1 mol % based on the amount of metal (ICP-MS analysis). As can be seen by the results shown in Table 1, the palladium hybrid material 3 was highly effective for a wide variety of substrates. Because the inherent catalytic properties of GO and rGO have been studied in a variety of processes,^{4a,19} control experiments using the rGO under exactly the same reaction conditions were carried out, showing that the palladium-free material was completely ineffective (entry 1). For the reaction carried out using complex 1, we obtained a moderate yield of ethylbenzene, whereas 3 produced a quantitative yield under the same reaction conditions (compare entries 2 and 5). These results suggest that the support provides a significant benefit in the catalytic hydrogenation reaction, most probably due to the surface area of rGO, which may facilitate the interaction between the substrates and the catalyst.²⁰ This “abnormal” enhancement in the activity of the immobilized catalyst onto the graphene material has already been observed before for the case of the hydrogenation of cyclohexene facilitated by a rhodium complex covalently supported onto graphene oxide.⁵ The NHC-Pd-rGO material, 3, is also very active in the hydrogenation of other terminal and internal alkenes (entries 6–10), also including nonaromatic ones (entry 10). The ICP-MS analysis after the experiment carried out with *trans*-stilbene as substrate (entry 8) accounts for 9.0 wt % of palladium, indicating negligible palladium leaching.

In order to determine if the process is homogeneously catalyzed by the molecular palladium complex, we performed the mercury-drop experiment for the reduction of styrene catalyzed by 1, and we observed that the reaction stopped upon addition of mercury (compare entries 2, 3, and 4, Table 1). It has to be taken into account that for this test to be effective, the addition of mercury has to be done after the catalyst has been

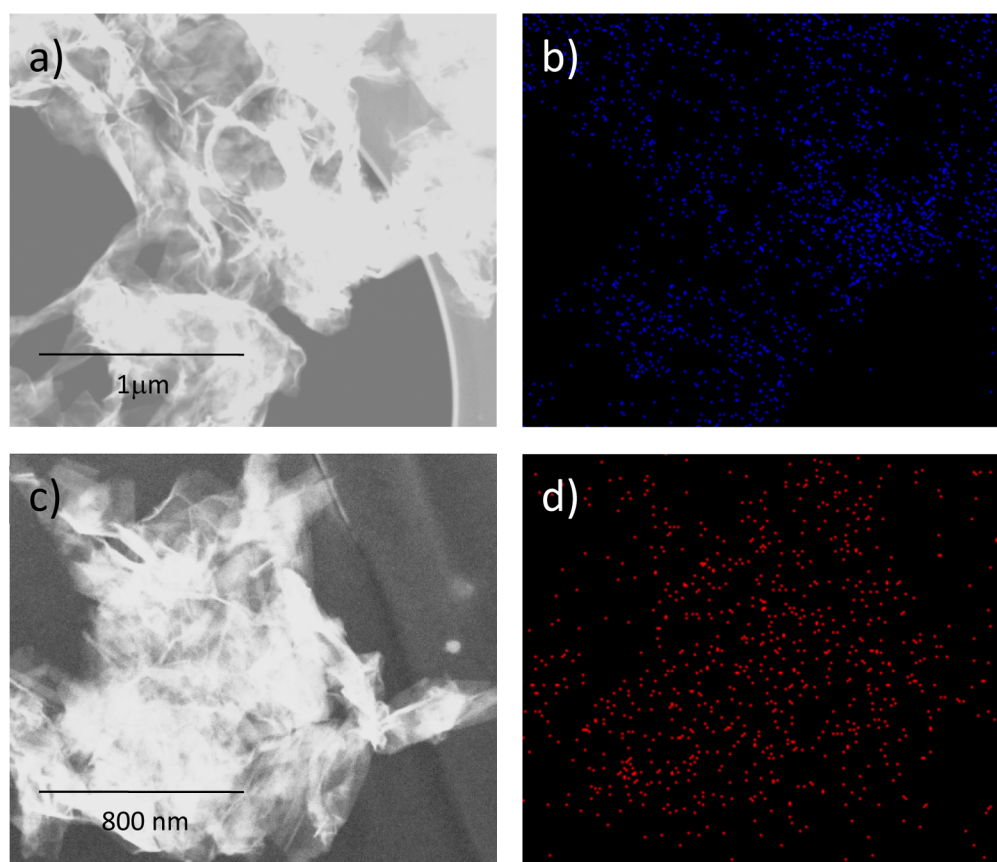


Figure 2. STEM images of NHC-Pd-rGO (**3**) (a), NHC-Ru-rGO (**4**) (c), and EDS elemental mapping image showing the homogeneous distribution of palladium (b) and ruthenium (d).

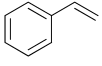
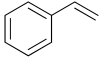
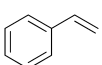
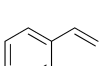
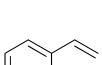
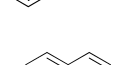
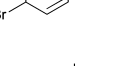
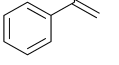
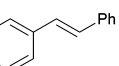
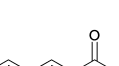
activated, and therefore the drop was added after 15 min of reaction. This result suggests that the reaction may be heterogeneously rather than homogeneously catalyzed and should imply that palladium nanoparticles are produced along the reaction course.²¹ In order to confirm this point, we also analyzed by HRTEM the NHC-Pd-rGO material, **3**, after being used in the reduction of styrene (Table 1, entry 5), and we observed a homogeneous distribution of palladium along the sample, together with the formation of small amounts of palladium nanoparticles. Very recent examples of NHC-based complexes covalently immobilized onto graphene oxide (GO) have also resulted in decomposition of the parent original complexes onto palladium nanoparticles, although the catalytic performances were maintained, and good recyclability could be achieved.²²

Catalyst **3** was also tested in the reduction of nitroarenes, a very interesting process due to the applications of functionalized anilines in the synthesis of pharmaceuticals and fine chemicals.²³ The results show that **3** is also an efficient catalyst for the reduction of nitroarenes in short times and low hydrogen pressures (Table 2). For this reaction, we also observed that rGO is completely inactive (entry 1), and that the molecular complex **1** was less active than the supported counterpart (entries 2–3), therefore suggesting that the rGO plays a positive role in the overall catalytic cycle, as we observed before. In a very recent work, palladium nanoparticles have also been supported onto graphene supports, by reduction of Pd(II) precursors, and the resulting materials have shown excellent activities in the reduction of alkenes and nitroarenes.²⁴

The oxidant-free oxidation of alcohols is a highly attractive process for the synthesis of carbonyl species and for the generation of molecular hydrogen from easily available alcohols.²⁵ Metal-based ruthenium catalysts have been widely used for this process.²⁶ The reactions were carried out in toluene, under aerobic conditions, Cs_2CO_3 , and a catalyst loading of 2 mol % based on metal amount (Table 3). The optimization of the reaction was carried out using 1-phenyl ethanol (entries 1–3) and benzyl alcohol (entries 4–7) as model substrates. Blank experiments on both substrates using rGO under the same reaction conditions, revealed that no oxidation occurs (entries 1 and 4). Oxidation of 1-phenyl ethanol and benzyl alcohol under homogeneous conditions using the molecular catalyst **2** afforded low yields of acetophenone (26%) and moderate yields of benzaldehyde (47%) (entries 2 and 5, respectively). When the oxidation reaction was carried out using the hybrid material NHC-Ru-rGO (**4**), the acetophenone yield increased up to 60% and >99% for the case of benzaldehyde (entries 3 and 7). These results suggest that immobilization of the molecular catalyst **2** on rGO provides a benefit in the catalytic process as previously observed in the case of the hydrogenation processes. Catalyst **4** was very effective in the oxidation of a wide set of benzyl alcohols, affording quantitative yields, regardless of the presence of electron-accepting or electron-donating substituents in the substrate (entries 8–11). For this process, we confirmed that the molecular complex **2** was the effective catalyst in the oxidation of benzyl alcohol, because the mercury-drop experiment resulted in no deactivation of the process, therefore suggesting that the reaction is homogeneously catalyzed

Table 1. Alkene Hydrogenation Using Molecular Hydrogen^[a]

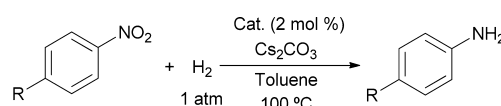
$$\text{R-CH=CH}_2 + \text{H}_2 \xrightarrow[\text{1 atm}]{\text{Cat. (1 mol \%), Cs}_2\text{CO}_3, \text{Toluene, 100 }^\circ\text{C}} \text{R-CH}_2\text{CH}_3$$

Entry	Catalyst	Substrate	Yield (%) ^b
1	rGO		0
2	1		60
3 ^[d]	1		80
4 ^[e]	1		62
5	NHC-Pd-rGO (3)		100
6	NHC-Pd-rGO (3)		88
7	NHC-Pd-rGO (3)		100
8	NHC-Pd-rGO (3)		100 ^c
9	NHC-Pd-rGO (3)		100
10	NHC-Pd-rGO (3)		100

^[a]Reactions were carried out with 0.3 mmol of alkene, Cs₂CO₃ (0.3 mmol), H₂ (1 atm), catalyst (1 mol %), 5 mL of toluene for 15 min at 100 °C. ^[b]Yields determined by GC analyses using anisole as internal standard. ^[c]Isolated yield. ^[d]Data after 30 min of reaction. ^[e]The reaction was allowed to proceed during 15 min, and then a mercury drop was added. The final yield is obtained after 15 more minutes of reaction.

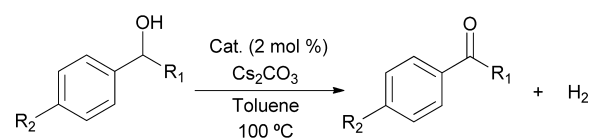
(entries 5–6). The HRTEM analysis of the catalyst NHC-Ru-rGO (**4**), after being used in the oxidation of benzyl-alcohol, revealed the absence of Ru-based nanoparticles in the solid, therefore confirming that the nature of the catalytic species for this system should be molecular.

In view of the good results obtained with the hybrid materials in catalysis, we decided to explore the catalyst stability by exploring their recyclability and activity in large-scale experiments. Recycling experiments of the palladium-containing catalyst **3** were carried out using styrene as model substrate

Table 2. Nitro Reduction Using Molecular Hydrogen^[a]

entry	catalyst	R	yield (%) ^[b]
1	rGO	H	0
2	1	H	50
3	NHC-Pd-rGO (3)	H	100
4	NHC-Pd-rGO (3)	CH ₃	100
5	NHC-Pd-rGO (3)	CH ₃ O	100 ^[c]

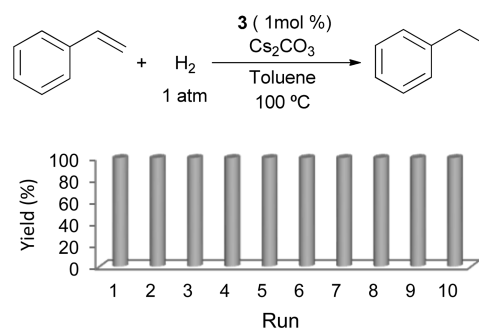
^[a]Reactions were carried out with 0.3 mmol of nitro compound, Cs₂CO₃ (0.3 mmol), H₂ (1 atm), catalyst (2 mol %), 5 mL of toluene for 2 h at 100 °C. ^[b]Yields determined by GC analyses using anisole as internal standard. ^[c]Isolated yield.

Table 3. Oxidant-Free Dehydrogenation of Alcohols^[a]

entry	catalyst	R ₁	R ₂	yield (%) ^[b]
1	rGO	CH ₃	H	0
2	2	CH ₃	H	26
3	NHC-Ru-rGO (4)	CH ₃	H	60
4	rGO	H	H	0
5	2	H	H	47
6 ^[c]	2	H	H	49
7	NHC-Ru-rGO (4)	H	H	100
8	NHC-Ru-rGO (4)	H	Cl	100
9	NHC-Ru-rGO (4)	H	NO ₂	100
10	NHC-Ru-rGO (4)	H	OMe	100
11	NHC-Ru-rGO (4)	H	CH ₃	100

^[a]Reactions were carried out with 0.3 mmol of alcohol, Cs₂CO₃ (0.3 mmol), catalyst (2 mol %), 5 mL of toluene for 12 h at 100 °C. ^[b]Yields determined by GC analyses using anisole as internal standard. ^[c]The reaction was allowed to proceed during 1 h, and then a mercury drop was added. The final yield is obtained after 11 more hours of reaction.

(Figure 3). The reaction conditions used in these experiments were the same as those described in the hydrogenation reactions, and the reaction progress was monitored by GC. After completion of each run (15 min), the reaction mixture was allowed to reach room temperature, and the solid catalyst was separated by centrifugation, washed with CH₂Cl₂, dried,

**Figure 3.** Recycling experiment of styrene hydrogenation using NHC-Pd-rGO (**3**).

and reused in the subsequent run. Interestingly, the base was only needed for the first run. This observation may be due to the transformation of the complex into the active catalytic species during the first run or simply to the adsorption of residual Cs_2CO_3 to the rGO surface, which avoided the need of further addition in the subsequent experiments. EDS analysis of NHC-Pd-rGO (3) after the 10th run revealed the presence of homogeneously distributed Cs, which may suggest that some base remains attached to the surface of the solid (Figure S13). Following this methodology, the palladium-containing catalyst 3 was reused up to 10 times without any decrease in activity, affording ethylbenzene in quantitative yield for each of the 10 runs. The ICP-MS analysis after the recycling experiments accounts for 8.5 wt % of palladium, indicating a total loss of 0.8 wt %, and thus 8.6% of the palladium is lost after 10 catalytic cycles. However, this small loss of percent of metal content may be due to the mass gain during the subsequent cycles due to the adsorption of substances from the catalyst reactions (we already mentioned that Cs_2CO_3 is adsorbed), so it may not be due to desorption or leaching of the metal complex. After the 10th experiment, a SEM image of the NHC-Pd-rGO (3) revealed that the morphology of rGO is maintained (Figure S6–S7). A deeper analysis by HRTEM showed that there is a well-dispersed palladium distribution, although the presence of some small (<8 nm diameter) palladium nanoparticles (Figure S12–S14) was detected.

The high activity of catalyst 3 was further analyzed in a large-scale experiment. The reaction was carried out using 2 mL of styrene (17.3 mmol) and a catalyst load of 0.01 mol % based on palladium (1.74×10^{-3} mmol). The reaction achieved quantitative yield after 20h, therefore achieving a maximum TON of 10,000. A recyclability study using these conditions reveals that the system is active at least for three runs without decrease in activity (Figure 4). The monitoring of the reaction

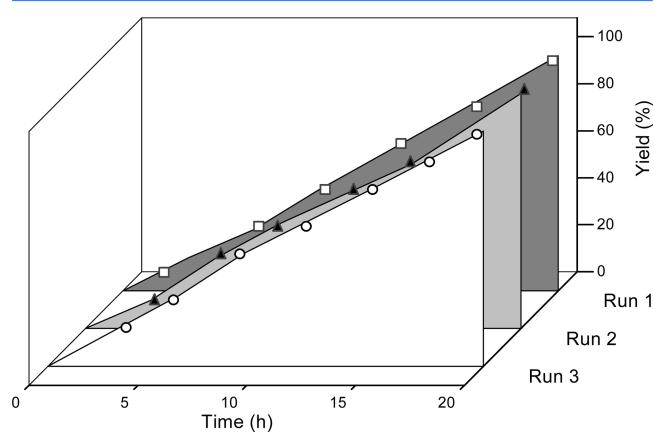


Figure 4. Recycling experiment of styrene hydrogenation using NHC-Pd-rGO (3) at a catalyst load of 0.01 mol %.

progress by GC indicates that the activity of catalyst 3 is maintained along the three consecutive runs (the accumulated TON is 30,000), therefore revealing that there is no trace of catalyst deactivation. A very interesting feature that is worth mentioning after evaluating these experiments, is the zero order dependence of the rate on the concentration of the substrate (styrene), as can be observed from the linear plots shown in Figure 4. Zero-order dependence on the concentration of the substrate is usually observed in heterogeneous hydrogenations of olefins and is interpreted to indicate that the surface of the

catalyst is saturated with the substrate,²⁷ and therefore suggests that in our case there is probably some interaction between the substrate and the support.

The recycling experiments for the ruthenium-containing catalyst 4, were performed by using benzyl alcohol as model substrate (Figure 5). The reactions were carried out using a

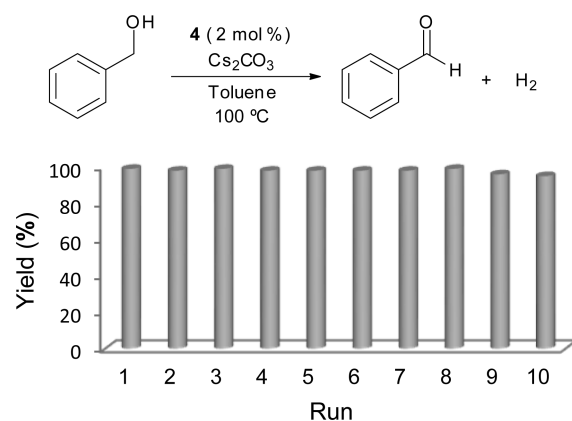


Figure 5. Recycling experiment of benzyl alcohol oxidation using NHC-Ru-rGO (4).

catalyst load of 2 mol %, at 100 °C and in the presence of Cs_2CO_3 (only in the first run). The mixture was allowed to react for 12h for each run. Then the catalyst was separated from the reaction mixture by centrifugation, washed, dried and replaced in the reaction vessel to be used in the subsequent run. As stated above, the fact that the base was only needed in the first cycle may indicate that either once the precatalyst has been transformed into its active form and that the active species is stable for recyclability during the subsequent runs, or that the base is adsorbed onto the solid support (as indicated by the detection of homogeneously distributed Cs by EDS analysis of the solid after the 10th run and therefore no further base is needed for the subsequent runs (Figure S13). Catalyst 4 was reused up to ten times without any decrease in activity, affording quantitative yields of benzaldehyde. The ICP-MS analysis after the recycling experiments accounts for 7.7 wt % of ruthenium, indicating that a total loss of 1.3 wt % and thus 14.4% of ruthenium is lost. However, as mentioned for the palladium supported catalyst, it is possible that this loss of percent of metal content is due to the mass gain during the subsequent cycles, rather than to leaching of the metal complex. The comparison of the SEM and HRTEM analysis of 4 before and after the recycling experiments revealed the same well-dispersed ruthenium distribution, without modification of the support morphology and the absence of ruthenium nanoparticles (Figures S8 – S9 and S15 – S17).

The large-scale experiment was carried out using 1 mL of benzyl alcohol (9.7 mmol) and a catalyst loading of 0.03 mol % based on ruthenium (3.0×10^{-3} mmol). The reaction yielded 75% of benzaldehyde after 24 h. As can be seen in Figure 6, NHC-Ru-rGO (4) could be reused up to three times, and the reaction profiles were identical in the first two cycles, therefore suggesting that the deactivation of the catalyst is negligible. In the third cycle, a slight decrease in catalyst activity is observed, and the reaction afforded a 65% yield in 24 h. This experiment is very interesting, because the reaction conditions used for this catalytic experiment show that the catalyst is using its full potential to achieve a 75% yield in the first cycle, therefore any

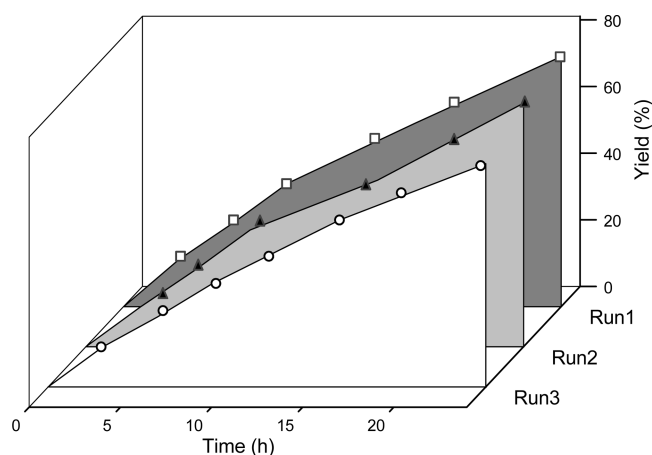


Figure 6. Recycling experiment of benzyl alcohol oxidation using NHC-Ru-rGO (4) at a catalyst load of 0.03 mol %.

minimum loss of catalyst or any deactivation should have measurable consequences in the recycling of the catalyst. Again, as can be observed from the linear plots depicted in Figure 5, the reaction shows quasi-zero-order dependence of the rate on the concentration of the substrate (benzyl alcohol), thus suggesting surface saturation due to the interaction between the substrate and the support.

In a parallel experiment, and in order to prove that the reaction was heterogeneously catalyzed, we performed a hot filtration experiment. This experiment was carried out using the general conditions described in Table 3 using benzyl alcohol as a substrate. After 6 h (GC yield 48%), the catalyst was filtered off at 100 °C. The filtrate was allowed to stir for 16 h under identical conditions, but GC analysis indicated that no further oxidation occurred (GC final yield is maintained in 48%). This experiment confirmed the absence of catalytic active species in solution due to ruthenium leaching or desorption of the molecular catalyst by the boomerang effect.²⁸ The boomerang effect consists of a release-and-return of the molecular complex from the support, therefore implying that the catalytic active species may be homogeneous in nature.²⁹ This observation contrasts with previously published results regarding the π -stacking between pyrene and carbon nanotubes, which is affected by the polarity of the solvent and by temperature.^{9b,30} For pyrene-containing complexes grafted onto graphene, it has also been published that desorption is temperature-dependent when polar organic solvents or water are used⁹ and that leaching is reduced when the metal complex is decorated with three pyrene tags.^{8b} In our case, and probably unexpectedly, we did not observe desorption of the molecular complexes 1 or 2 in polar or nonpolar solvents such as dichloromethane, acetone, toluene, or *i*-propanol.

CONCLUSIONS

In summary, we have prepared palladium and ruthenium molecular complexes containing an N-heterocyclic carbene ligand with a pyrene tag. The two complexes have been anchored on the surface of rGO by noncovalent interactions under mild reaction conditions yielding the hybrid materials NHC-Pd-rGO (3) and NHC-Ru-rGO (4). This modular methodology allows incorporation of well-defined molecular complexes onto chemical derived graphenes (CDGs), where the properties of the complex are not altered by the effect of the immobilization. The catalytic properties of the molecular

complexes and hybrid materials have been studied in the hydrogenation of alkenes and alcohol oxidation. The results show that the catalytic properties are improved in the hybrid materials, compared to the catalytic outcomes provided by the homogeneous analogues. The catalyst stability was analyzed by recyclability, hot filtration, and large-scale experiments. Although the activity of the palladium catalyst may be ascribed to the formation of palladium nanoparticles, we confirmed the molecular nature of the ruthenium-based catalysts, therefore constituting a unique example of a molecular catalyst noncovalently supported onto a graphene derivative. Both catalysts 3 and 4 were reused up to 10 times without any decrease in activity affording quantitative yield of products. Probably more revealing is the fact that the catalysts used in large-scale experiments could be recycled, with catalyst loadings of 0.01 and 0.03 mol % for 3 and 4, respectively. Even under these reaction conditions, the catalysts could be reused up to three times without loss of activity and display the same reaction profiles, therefore indicating that catalyst deactivation is negligible. The hot filtration experiment reveals that the catalysis is heterogeneous in nature without any detectable leaching or boomerang effect.

We strongly believe that the simplicity of the design of these heterogeneous catalytic systems, in combination with its great catalytic performance and recyclability, may inspire future research in the field of catalyst heterogenization. To the best of our knowledge, this is the first example of a supported NHC-molecular catalyst onto a graphene derivative, and we demonstrated its great potential in practical applications.

EXPERIMENTAL SECTION

All manipulations were carried out under nitrogen using standard Schlenk techniques and high vacuum, unless otherwise stated. Anhydrous solvents were obtained using a solvent purification system (SPS M BRAUN) or purchased from commercial suppliers and degassed prior to use by purging with dry nitrogen and kept over molecular sieves. Reduced graphene oxide and the other reagents were used as received from commercial suppliers. NMR spectra were recorded on Varian Inova spectrometers operating at 300 or 500 MHz (¹H NMR) and 75 and 125 MHz (¹³C NMR), respectively. Elemental analyses were carried out in an EA 1108 CHNS-O Carlo Erba analyzer. Electrospray mass spectra (ESI-MS) were recorded on a MicromassQuattro LC instrument, and nitrogen was employed as drying and nebulizing gas. Raman spectra were acquired on a JASCO NRS-3100 dispersive spectrometer. Infrared spectra (FTIR) were recorded on a JASCO FTIR-6200 spectrometer with a spectral window of 4000–500 cm⁻¹. Scanning electron micrographs were taken with a field emission gun scanning electron microscope (FEG-SEM) model JEOL 7001F, equipped with a spectrometer of energy dispersion of X-ray (EDX) from Oxford instruments. High-resolution transmission electron microscopy images (HRTEM) and high-angle annular dark-field HAADF-STEM images of the samples were obtained using a Jem-2100 LaB6 (JEOL) transmission electron microscope coupled with an INCA Energy TEM 200 (Oxford) energy-dispersive X-ray spectrometer (EDX) operating at 200 kV. The UV–vis spectra were recorded between 200 and 800 nm by a Cary 300 Bio UV–vis Varian spectrophotometer.

The determination of the metal loading was done by ICP–MS Agilent 7500 CX. The digestion of the samples was carried out under reflux of a mixture of concentrated nitric and hydrochloric acids (3:1) for 12 h. The digestion of the samples

after the recycling experiments were carried out after several washes with milli-Q water (10 × 10 mL).

Synthesis of Imidazolium Salt A. 1-(Bromomethyl)pyrene (1 g, 3.39 mmol) and 1-methyl imidazole (0.28 mL, 3.39 mmol) were refluxed under nitrogen in dry THF (10 mL) for 16 h. The resulting suspension was filtered yielding a white precipitate which was washed with diethyl ether (2 × 10 mL). Yield: 1.2 g (96%). ¹H NMR (300 MHz, DMSO): δ 9.21 (s, 1H, NCHN), 8.51–8.08 (m, 9H, CH_{Ar}), 7.87 (d, ³J_{H,H} = 1.7 Hz, 1H, CH_{imidazole}), 7.73 (d, ³J_{H,H} = 1.7 Hz, 1H, CH_{imidazole}), 6.23 (s, 2H, NCH₂-), 3.82 (s, 3H, NCH₃). ¹³C{¹H} NMR (75 MHz, DMSO): δ 137.1(NCHN), [131.9, 131.1, 130.6, 129.2, 129.1, 128.6, 128.4, 127.8, 127.7, 127.1, 126.4, 126.2, 125.6, 124.5, 124.3, 124.1, 123.1, 122.8] (CH_{Ar}, CH_{imidazole}), 50.4 (NCH₂-), 36.3 (NCH₃). Anal. Calcd for C₂₁H₁₇N₂Br·H₂O (395.29): C, 63.80; H, 4.84; N, 7.08. Found: C, 64.23; H, 5.21; N, 6.94. Electrospray MS (Cone 20 V) (*m/z*, fragment): 297.4 [M]⁺. HRMS ESI-TOF-MS (positive mode): [M]⁺ monoisotopic peak 297.1389; calcd 297.1392, ε_r 1 ppm.

Synthesis of 1. Imidazolium salt A (127 mg, 0.334 mmol), [Pd(dmba)OAc]₂ (100 mg, 0.167 mmol), and KBr (40 mg, 0.334 mmol), were refluxed under nitrogen in 10 mL of acetonitrile for 16 h. The resulting suspension was filtered through Celite, and the solvent was evaporated under reduced pressure. The crude solid was purified by column chromatography. Elution with a mixture DCM/acetone 9:1 afforded the separation of a yellowish band containing the desired product. Precipitation with DCM/hexanes afforded an analytically pure yellow solid. Yield: 128 mg (60%). ¹H NMR (300 MHz, CDCl₃): δ 8.38 (d, ³J_{H,H} = 9.3 Hz, 1H, CH_{Arpyrene}), 8.19–7.89 (m, 8H, CH_{Arpyrene}), 7.09–7.01 (m, 2H, CH_{Arphenyl}), 6.87 (td, ³J_{H,H} = 7.4, 2.8 Hz, 1H, CH_{Arphenyl}), 6.77 (d, ³J_{H,H} = 1.9 Hz, 1H, CH_{imidazole}), 6.43 (d, ³J_{H,H} = 1.9 Hz, 1H, CH_{imidazole}), 6.31 (d, ³J_{H,H} = 14.5 Hz, 1H, N_{imidazole}CH_aH_b-), 6.18 (d, ³J_{H,H} = 14.5 Hz, 1H, N_{imidazole}CH_aH_b-), 6.15 (d, ³J_{H,H} = 6.9 Hz, 1H, CH_{Arphenyl}), 4.01 (d, ³J_{H,H} = 14.0 Hz, 1H, N_{amine}CH_aH_b-), 3.99 (s, 3H, N_{imidazole}CH₃), 3.87 (d, ³J_{H,H} = 14.0 Hz, 1H, N_{amine}CH_aH_b-), 2.95 (s, 3H, N_{amine}CH₃), 2.92 (s, 3H, N_{amine}CH₃). ¹³C{¹H} NMR (75 MHz, CDCl₃): δ 172.9 (C_{carbene} - Pd), [150.3, 148.7, 135.6, 131.8, 131.1, 130.7, 129.7, 128.8, 128.6, 128.1, 127.9, 127.2, 126.1, 125.7, 125.6, 125.5, 124.9, 124.7, 124.5, 124.1, 123.7, 122.5, 122.1, 120.3] (CH_{Ar}, CH_{imidazole}), 72.2 (N_{amine}CH₂-), 53.7 (N_{imidazole}CH₂-), [51.2, 50.6] (N_{amine}CH₃), 38.7 (NCH₃). Anal. Calcd for C₃₀H₂₈N₃PdBr·H₂O (634.90): C, 56.75; H, 4.76; N, 6.62. Found: C, 56.93; H, 5.09; N, 6.35. Electrospray MS (Cone 20 V) (*m/z*, fragment): 536.3 [M - Br]⁺. HRMS ESI-TOF-MS (positive mode): [M - Br]⁺ monoisotopic peak 536.1333; calcd 536.1330, ε_r 0.6 ppm.

Synthesis of 2. In a round-bottom flask were mixed, under exclusion of light, the imidazolium salt A (124.2 mg, 0.326 mmol) and Ag₂O (75.5 mg, 0.326 mmol) in 10 mL of acetonitrile, and the suspension was refluxed for 5 h. Then [RuCl₂(η⁶-p-cymene)]₂ (100 mg, 0.163 mmol) and KCl (243 mg, 3.25 mmol) were added, and the reaction mixture was stirred at room temperature for 15 h. The resulting suspension was filtered through Celite, and the solvent was evaporated under reduced pressure. The crude solid was purified by column chromatography. Elution with a mixture of DCM/acetone (9:2) afforded the separation of an orange band containing the desired product. Precipitation with DCM/diethyl ether afforded an analytically pure orange solid. Yield: 120 mg, 61%. ¹H NMR (300 MHz, CDCl₃): δ 8.38 (d, ³J_{H,H} =

9.3 Hz, 1H, CH_{Ar}), 8.27–8.00 (m, 7H, CH_{Ar}), 7.70 (d, ³J_{H,H} = 8.0 Hz, 1H, CH_{Ar}), 7.04 (d, ³J_{H,H} = 1.9 Hz, 1H, CH_{imidazole}), 6.92 (d, ³J_{H,H} = 1.8 Hz, 1H, CH_{imidazole}), 6.75–6.33 (broad s, 2H, NCH₂-), 5.26 (broad s, 2H, CH_{p-cym}), 4.89 (d, ³J_{H,H} = 5.9 Hz, 2H, CH_{p-cym}), 4.11 (s, 3H, NCH₃), 2.98–2.76 (m, 1H, CH_{isopp-cym}), 2.02 (s, 3H, CH_{3p-cym}), 1.18 (d, ³J_{H,H} = 6.7 Hz, 6H, CH_{3isop p-cym}). ¹³C{¹H} NMR (75 MHz, CDCl₃): δ 174.8 (C_{carbene} - Ru), [131.3, 131.1, 130.8, 130.8, 128.7, 128.4, 127.8, 127.2, 126.3, 125.6, 125.6, 124.9, 124.7, 124.6, 124.6, 123.8, 123.6, 122.4] (CH_{Ar}, CH_{imidazole}), [108.1, 98.9] (C_{q-p-cym}), [85.1, 82.4] (CH_{p-cym}), 52.8 (NCH₂-), 39.9 (NCH₃), 30.7 (CH_{isopp-cym}), 22.3 (CH_{3p-cym}), 18.7 (CH_{3isop p-cym}). Anal. Calcd for C₃₁H₃₀N₂RuCl₂ (620.58): C, 59.99; H, 5.19; N, 4.51. Found: C, 60.38; H, 5.43; N, 4.62. Electrospray MS (Cone 20 V) (*m/z*, fragment): 567.2 [M - Cl]⁺. HRMS ESI-TOF-MS (positive mode): [M - Cl]⁺ monoisotopic peak 567.1144; calcd 567.1146, ε_r 0.4 ppm.

Preparation of NHC-M-rGO. In a round-bottom flask were introduced 90 mg of rGO and 10 mL of DCM. The suspension was sonicated for 30 min. Then, 10 mg of the corresponding metal complex 1 or 2 was added. The suspension was stirred at room temperature for 10 h until the solution become clear. The black solid was filtrated and washed with 2 × 15 mL of DCM, affording the resulting product as a black solid. The filtrates were combined and evaporated to dryness under reduced pressure. Unsupported complex 1 or 2 was analyzed by ¹H NMR using anisole as internal standard. Integration of the characteristic signal of anisole (-OMe) versus (NCH₂-Pyr) reveals the amount complex that has been deposited on the rGO. The exact amount of complex supported was determined by ICP-MS analysis.

General Procedure for Alkene Reductions. Molecular hydrogen was added with a balloon filled with 1 atm of H₂ to a mixture of alkene (0.3 mmol), Cs₂CO₃ (0.3 mmol), and NHC-Pd-rGO (3 × 10⁻³ mmol, based on metal) in toluene (5 mL). The system was then evacuated and backfilled with H₂ in cycles for three times before putting the reaction vessel in an oil bath at 100 °C for 15 min. Yields were determined by GC analyses using anisole (0.3 mmol) as internal standard. Products were identified according to spectroscopic data of the commercially available compounds.

Recycling Experiments. The hydrogenation reaction was carried out under identical reaction conditions as described in the alkene reduction procedure. After completion of each run (15 min), the reaction mixture was allowed to reach room temperature and was centrifuged. The remaining solid was washed thoroughly with CH₂Cl₂ (5 × 10 mL), dried, and reused in the following run. The base was only added in the first run.

Large-Scale Recycling Experiments. Molecular hydrogen was added with a balloon filled with 1 atm of H₂ to a mixture of styrene (2 mL, 17.3 mmol), Cs₂CO₃ (2.8 g, 8.65 mmol), anisole as internal standard (1.9 mL, 17.3 mmol), and NHC-Pd-rGO (1.74 × 10⁻³ mmol, based on metal) in toluene (20 mL). The system was then evacuated and backfilled with H₂ in cycles for three times before putting the reaction vessel in an oil bath at 100 °C. Reaction monitoring, yields, and conversions were determined by GC analyses. After completion of each run (20 h), the reaction mixture was allowed to reach room temperature and was centrifuged. The remaining solid was washed thoroughly with CH₂Cl₂ (5 × 10 mL), dried, and reused in the following run. The base was only added in the first run.

General Procedure for Nitroarene Reductions. Molecular hydrogen was added with a balloon filled with 1 atm of H₂ to a mixture of nitroarene (0.3 mmol), Cs₂CO₃ (0.3 mmol), anisole as internal standard (0.3 mmol), and NHC-Pd-rGO (6 × 10⁻³ mmol, based on metal) in toluene (5 mL). The system was then evacuated and backfilled with H₂ in cycles for three times before putting the reaction vessel in an oil bath at 100 °C for 2 h. Yields were determined by GC analyses using anisole (0.3 mmol) as internal standard. Products were identified according to spectroscopic data of the commercially available compounds.

General Procedure for Alcohol Oxidations. In a round-bottom flask a mixture of the alcohol (0.3 mmol), Cs₂CO₃ (0.3 mmol), and the NHC-Ru-rGO (6 × 10⁻³ mmol, based on metal) was refluxed in toluene (4 mL) for 12 h. Yields were determined by GC analyses using anisole (0.3 mmol) as internal standard. Products were identified according to spectroscopic data of the commercially available compounds.

Recycling Experiments. The recycling of benzyl alcohol oxidation was carried out under identical reaction conditions as described before. After completion of each run (12 h), the reaction mixture was allowed to reach room temperature and was centrifuged. The remaining solid was washed thoroughly with CH₂Cl₂ (5 × 10 mL), dried, and reused in the following run. The base was only added in the first run.

Large-Scale Recycling Experiments. In a round-bottom flask, a mixture of benzyl alcohol (1 mL, 9.66 mmol), Cs₂CO₃ (1.5 g, 4.83 mmol), anisole as internal standard (1 mL, 9.66 mmol), and the NHC-Ru-rGO (3 × 10⁻³ mmol, based on metal) was refluxed in toluene (10 mL) for 24 h. Reaction monitoring, yields, and conversions were determined by GC analyses. After completion of each run (24 h), the reaction mixture was allowed to reach room temperature and was centrifuged. The remaining solid was washed thoroughly with CH₂Cl₂ (5 × 10 mL), dried, and reused in the following run. The base was only added in the first run.

Hot Filtration Test. This experiment was carried out under identical reaction conditions as earlier described. After 6 h (yield 48%), the catalyst was filtered off at the reaction temperature (100 °C), and the solid free filtrate was allowed to stir for 16 h under identical reaction conditions. GC analysis monitoring indicated that no further oxidation of benzyl alcohol occurred (GC final yield 48%).

■ ASSOCIATED CONTENT

● Supporting Information

Full characterization of molecular complexes and hybrid materials including high-resolution mass spectroscopy, NMR, X-ray crystal structure, UV-vis, FTIR, and Raman spectroscopy, as well as microscopy SEM and HRTEM images. This material is available free of charge via the Internet at <http://pubs.acs.org>.

■ AUTHOR INFORMATION

Corresponding Authors

*E-mail: jmata@uji.es.

*E-mail: eperis@uji.es.

Notes

The authors declare no competing financial interest.

■ ACKNOWLEDGMENTS

Dedicated to Prof. Pascual Lahuerta, on the occasion of his 70th birthday. We thank the financial support from the Ministerio de Ciencia e Innovación of Spain (CTQ2011-24055/BQU). We would also like to thank the Generalitat Valenciana for a fellowship to S.S. The authors are grateful to the Serveis Centrals d'Instrumentació Científica (SCIC) of the Universitat Jaume I for providing us with spectroscopic and X-ray facilities.

■ ABBREVIATIONS

rGO, reduced graphene oxide; GO, graphene oxide; dmab, cyclo-orthometalated *N,N*-dimethyl benzylamine; NHC, N-heterocyclic carbene ligand; CDGs, chemically derived graphenes

■ REFERENCES

- (1) Cole-Hamilton, D. J. *Science* **2003**, *299*, 1702–1706.
- (2) (a) Jones, C. W. *Top. Catal.* **2010**, *53*, 942–952. (b) Wang, Z.; Chen, G.; Ding, K. L. *Chem. Rev.* **2009**, *109*, 322–359. (c) Gladysz, J. A. *Chem. Rev.* **2002**, *102*, 3215–3216. (d) Fraile, J. M.; Garcia, J. I.; Mayoral, J. A. *Chem. Rev.* **2009**, *109*, 360–417. (e) Coperet, C.; Chabanas, M.; Saint-Arroman, R. P.; Basset, J. M. *Angew. Chem., Int. Ed.* **2003**, *42*, 156–181. (f) Bond, G. C. *Chem. Soc. Rev.* **1991**, *20*, 441–475.
- (3) Castro Neto, A. H.; Guinea, F.; Peres, N. M. R.; Novoselov, K. S.; Geim, A. K. *Rev. Mod. Phys.* **2009**, *81*, 109–162.
- (4) (a) Machado, B. F.; Serp, P. *Catal. Sci. Technol.* **2012**, *2*, 54–75. (b) Pyun, J. *Angew. Chem., Int. Ed.* **2011**, *50*, 46–48. (c) Su, C. L.; Loh, K. P. *Acc. Chem. Res.* **2013**, *46*, 2275–2285. (d) Luo, B.; Liu, S. M.; Zhi, L. J. *Small* **2012**, *8*, 630–646.
- (5) Zhao, Q.; Chen, D.; Li, Y.; Zhang, G.; Zhang, F.; Fan, X. *Nanoscale* **2013**, *5*, 882–885.
- (6) (a) Eda, G.; Chhowalla, M. *Adv. Mater.* **2010**, *22*, 2392–2415. (b) Podeszwa, R. J. *Chem. Phys.* **2010**, *132*, 044704. (c) Pan, B.; Xing, B. S. *Environ. Sci. Technol.* **2008**, *42*, 9005–9013. (d) Chen, J. Y.; Chen, W.; Zhu, D. *Environ. Sci. Technol.* **2008**, *42*, 7225–7230. (e) Muller, S.; Totsche, K. U.; Kogel-Knabner, I. *Eur. J. Soil Sci.* **2007**, *58*, 918–931. (f) Balapanuru, J.; Yang, J.-X.; Xiao, S.; Bao, Q.; Jahan, M.; Polavarapu, L.; Wei, J.; Xu, Q.-H.; Loh, K. P. *Angew. Chem., Int. Ed.* **2010**, *49*, 6549–6553.
- (7) (a) Sun, Y. B.; Yang, S. B.; Zhao, G. X.; Wang, Q.; Wang, X. K. *Chem.—Asian J.* **2013**, *8*, 2755–2761. (b) Yang, K.; Wang, X. L.; Zhu, L. Z.; Xing, B. S. *Environ. Sci. Technol.* **2006**, *40*, 5804–5810. (c) Chefetz, B.; Deshmukh, A. P.; Hatcher, P. G.; Guthrie, E. A. *Environ. Sci. Technol.* **2000**, *34*, 2925–2930. (d) Mao, X.; Su, H.; Tian, D.; Li, H.; Yang, R. *ACS Appl. Mater. Interfaces* **2013**, *5*, 592–597. (e) Qu, S.; Li, M.; Xie, L.; Huang, X.; Yang, J.; Wang, N.; Yang, S. *ACS Nano* **2013**, *7*, 4070–4081.
- (8) (a) Le Goff, A.; Reuillard, B.; Cosnier, S. *Langmuir* **2013**, *29*, 8736–8742. (b) Mann, J. A.; Rodriguez-Lopez, J.; Abruna, H. D.; Dichtel, W. R. *J. Am. Chem. Soc.* **2011**, *133*, 17614–17617.
- (9) (a) Keller, M.; Colliere, V.; Reiser, O.; Caminade, A.-M.; Majoral, J.-P.; Ouali, A. *Angew. Chem., Int. Ed.* **2013**, *52*, 3626–3629. (b) Wittmann, S.; Schaetz, A.; Grass, R. N.; Stark, W. J.; Reiser, O. *Angew. Chem., Int. Ed.* **2010**, *49*, 1867–1870.
- (10) (a) Georgakilas, V.; Otyepka, M.; Bourlinos, A. B.; Chandra, V.; Kim, N.; Kemp, K. C.; Hobza, P.; Zboril, R.; Kim, K. S. *Chem. Rev.* **2012**, *112*, 6156–6214. (b) Rodriguez-Perez, L.; Angeles Herranz, M.; Martin, N. *Chem. Commun.* **2013**, *49*, 3721–3735.
- (11) (a) Herrmann, W. A. *Angew. Chem., Int. Ed.* **2002**, *41*, 1290–1309. (b) Herrmann, W. A.; Elison, M.; Fischer, J.; Kocher, C.; Artus, G. R. J. *Angew. Chem., Int. Ed.* **1995**, *34*, 2371–2374. (c) Bourissou, D.; Guerret, O.; Gabbai, F. P.; Bertrand, G. *Chem. Rev.* **2000**, *100*, 39–91. (d) Diez-Gonzalez, S.; Nolan, S. P. *Coord. Chem. Rev.* **2007**, *251*, 874–883.
- (12) Janiak, C. *J. Chem. Soc., Dalton Trans.* **2000**, 3885–3896.

- (13) Merces, L.; Neels, A.; Albrecht, M. *Dalton Trans.* **2008**, 5570–5576.
- (14) (a) Ehli, C.; Guldi, D. M.; Herranz, M. A.; Martin, N.; Campidelli, S.; Prato, M. *J. Mater. Chem.* **2008**, *18*, 1498–1503. (b) Herranz, M. A.; Ehli, C.; Campidelli, S.; Gutierrez, M.; Hug, G. L.; Ohkubo, K.; Fukuzumi, S.; Prato, M.; Martin, N.; Guldi, D. M. *J. Am. Chem. Soc.* **2008**, *130*, 66–73. (c) Kavakka, J. S.; Heikkinen, S.; Kilpelainen, I.; Mattila, M.; Lipsanen, H.; Helaja, J. *Chem. Commun.* **2007**, 519–521.
- (15) (a) Ferrari, A. C.; Meyer, J. C.; Scardaci, V.; Casiraghi, C.; Lazzeri, M.; Mauri, F.; Piscanec, S.; Jiang, D.; Novoselov, K. S.; Roth, S.; Geim, A. K. *Phys. Rev. Lett.* **2006**, *97*, 187401. (b) Ferrari, A. C.; Robertson, J. *Phys. Rev. B* **2000**, *61*, 14095–14107.
- (16) Malard, L. M.; Pimenta, M. A.; Dresselhaus, G.; Dresselhaus, M. S. *Phys. Rep.* **2009**, *473*, 51–87.
- (17) (a) Clapham, S. E.; Hadzovic, A.; Morris, R. H. *Coord. Chem. Rev.* **2004**, *248*, 2201–2237. (b) Cui, X. H.; Burgess, K. *Chem. Rev.* **2005**, *105*, 3272–3296.
- (18) (a) Bertoli, M.; Choualeb, A.; Lough, A. J.; Moore, B.; Spasyuk, D.; Gusev, D. G. *Organometallics* **2011**, *30*, 3479–3482. (b) Nielsen, M.; Kammer, A.; Cozzula, D.; Junge, H.; Gladiali, S.; Beller, M. *Angew. Chem., Int. Ed.* **2011**, *50*, 9593–9597.
- (19) (a) Dreyer, D. R.; Jia, H.-P.; Bielawski, C. W. *Angew. Chem., Int. Ed.* **2010**, *49*, 6813–6816. (b) Huang, C.; Li, C.; Shi, G. *Energy Environ. Sci.* **2012**, *5*, 8848–8868.
- (20) Gao, Y.; Ma, D.; Wang, C.; Guan, J.; Bao, X. *Chem. Commun.* **2011**, *47*, 2432–2434.
- (21) Crabtree, R. H. *Chem. Rev.* **2012**, *112*, 1536–1554.
- (22) (a) Shang, N.; Gao, S.; Feng, C.; Zhang, H.; Wang, C.; Wang, Z. *RSC Adv.* **2013**, *3*, 21863–21868. (b) Movahed, S. K.; Esmatpoursalmani, R.; Bazgir, A. *RSC Adv.* **2014**, *4*, 14586–14591.
- (23) (a) Blaser, H.-U. *Science* **2006**, *313*, 312–313. (b) Siegrist, U.; Baumeister, P.; Blaser, H. U.; Studer, M. In *The Selective Hydrogenation of Functionalized Nitroarenes: New Catalytic Systems*, Herkes, F. E., Ed.; Marcel Dekker, Inc.: New York, 1998; Vol. 75, pp 207–219.
- (24) (a) Linhardt, R.; Kainz, Q. M.; Grass, R. N.; Stark, W. J.; Reiser, O. *RSC Adv.* **2014**, *4*, 8541–8549. (b) Kainz, Q. M.; Linhardt, R.; Grass, R. N.; Vilé, G.; Pérez-Ramirez, J.; Stark, W. J.; Reiser, O. *Adv. Funct. Mater.* **2014**, *24*, 2020–2027.
- (25) Adair, G. R. A.; Williams, J. M. J. *Tetrahedron Lett.* **2005**, *46*, 8233–8235.
- (26) (a) Blum, Y.; Czarkie, D.; Rahamim, Y.; Shvo, Y. *Organometallics* **1985**, *4*, 1459–1461. (b) Shvo, Y.; Czarkie, D.; Rahamim, Y.; Chodosh, D. F. *J. Am. Chem. Soc.* **1986**, *108*, 7400–7402. (c) Spasyuk, D.; Gusev, D. G. *Organometallics* **2012**, *31*, 5239–5242. (d) Hollmann, D.; Baehn, S.; Tillack, A.; Beller, M. *Angew. Chem., Int. Ed.* **2007**, *46*, 8291–8294. (e) Prades, A.; Peris, E.; Albrecht, M. *Organometallics* **2011**, *30*, 1162–1167.
- (27) (a) Kung, H. H.; Pellet, R. J.; Burwell, R. L. *J. Am. Chem. Soc.* **1976**, *98*, 5603–5611. (b) Lee, T. R.; Whitesides, G. M. *Acc. Chem. Res.* **1992**, *25*, 266–272. (c) Zaera, F. *Prog. Surf. Sci.* **2001**, *69*, 1–98. (d) Pomogailo, A. D. *Catalysis by Polymer-Immobilized Metal Complexes*; Gordon and Breach Science Publishers: Amsterdam, 1998.
- (28) (a) Clavier, H.; Caijo, F.; Borre, E.; Rix, D.; Boeda, F.; Nolan, S. P.; Mauduit, M. *Eur. J. Org. Chem.* **2009**, 4254–4265. (b) Clavier, H.; Nolan, S. P.; Mauduit, M. *Organometallics* **2008**, *27*, 2287–2292. (c) Kingsbury, J. S.; Harrity, J. P. A.; Bonitatebus, P. J.; Hoveyda, A. H. *J. Am. Chem. Soc.* **1999**, *121*, 791–799.
- (29) Vriamont, C.; Devillers, M.; Riant, O.; Hermans, S. *Chem.—Eur. J.* **2013**, *19*, 12009–12017.
- (30) (a) Liu, G.; Wu, B.; Zhang, J.; Wang, X.; Shao, M.; Wang, J. *Inorg. Chem.* **2009**, *48*, 2383–2390. (b) Schaetz, A.; Reiser, O.; Stark, W. J. *Chem.—Eur. J.* **2010**, *16*, 8950–8967.